1-14-2022

Applications of Stretching Technique and Time Window Effects on Ultrasonic Velocity Monitoring in Concrete

Bibo Zhong

Jinying Zhu

applied sciences

MDPI

Article

Applications of Stretching Technique and Time Window Effects on Ultrasonic Velocity Monitoring in Concrete

Bibo Zhong and Jinying Zhu *

Department of Civil and Environmental Engineering, University of Nebraska-Lincoln, 1110 S 67th St., Omaha, NE 68182, USA; bbzhong@huskers.unl.edu

* Correspondence: jyzhu@unl.edu

Abstract: Coda wave interferometry (CWI) has been used to measure the relative wave-velocity change (dV/V) caused by small changes in materials. This study uses the stretching processing technique which has been used for CWI analysis to investigate velocity changes of direct longitudinal (P) wave, direct shear (S) wave, and coda wave in concrete by choosing different time windows of ultrasonic signals. It is found that the obtained wave-velocity change depends on the time window position, because the relative contribution of P wave and S wave is different in each signal window. This paper presents three experimental scenarios of velocity change in concrete: early-age hydration, temperature change, and uniaxial loading. In early-age concrete, the S wave has a larger relative velocity change than the P wave, which is consistent with the microstructure development due to the hydration process. Temperature change causes a larger dV/V on the P wave than on the S wave, and the difference between P and S wave-velocity changes may be used to determine nonlinear elastic constants of materials. In the uniaxial loading experiment, analysis of the direct P wave can distinguish the acoustoelastic effects in the stress direction and the non-stress direction, which may potentially be used for stress evaluation in prestressed structures. However, the coda wave does not show this directional property to stress due to multiple scattering in the medium.

Keywords: stretching technique; coda wave interferometry (CWI); hydration; temperature; uniaxial loading; nondestructive evaluation; concrete

Citation: Zhong, B.; Zhu, J. Applications of Stretching Technique and Time Window Effects on Ultrasonic Velocity Monitoring in Concrete. *Appl. Sci.* **2022**, *12*, 7130. https://doi.org/10.3390/app12147130

Academic Editors: Yanhua Sun and Shiwei Liu

Received: 14 May 2022
Accepted: 12 July 2022
Published: 14 July 2022

1. Introduction

An ultrasonic coda wave is the tail part of a wave signal corresponding to the diffuse wave field. Because a coda wave is scattered and reflected multiple times in a medium, it has a high sensitivity to minor changes in material, either caused by a uniform property change or localized scatters. The time-lapse changes in the coda wave are typically calculated using coda wave interferometry (CWI) [1–3] by cross-correlating the disturbed and reference signals.

The CWI analysis evaluates the relative wave-velocity change dV/V between two coda wave signals by measuring the relative time shift dt/t, which can be estimated in two ways: doublet method [1] and stretching method [4]. The doublet method measures time shifts dt of many short segments at times t and then evaluates the relative time shift dt/t. The stretching method assumes a uniform change of wave velocity in the medium so that the perturbed signal is a stretched or compressed version of the reference signal. Hadziioannou et al. [5] measured temperature-induced velocity change in concrete and found that the stretching method gives stable results even for signals with a low signal-to-noise ratio (S/N). Because this study will analyze short time windows in a signal, only the stretching method will be used in the following analysis.

In the stretching analysis, the perturbed signal S_1 is interpolated at times $t(1+\varepsilon)$ with a stretching factor ε to obtain S_1', and then compared with the reference signal S_0 by calculating the cross-correlation coefficient (CC):

$$CC(\varepsilon) = \frac{\int_{t_1}^{t_2} S_1[t(1+\varepsilon)]S_0[t]dt}{\sqrt{\int_{t_1}^{t_2} S_1^2[t(1+\varepsilon)]dt \int_{t_1}^{t_2} S_0^2[t]dt}} \quad (1)$$

where $[t_1, t_2]$ is the selected time window for calculation. The stretching parameter ε_{max} that maximizes the cross-correlation coefficient is regarded as the relative time shift $-dt/t$, and then the relative wave-velocity change $dV/V = -dt/t = \varepsilon_{max}$ [1,4]. Figure 1 illustrates the stretching technique on two ultrasonic waveforms.

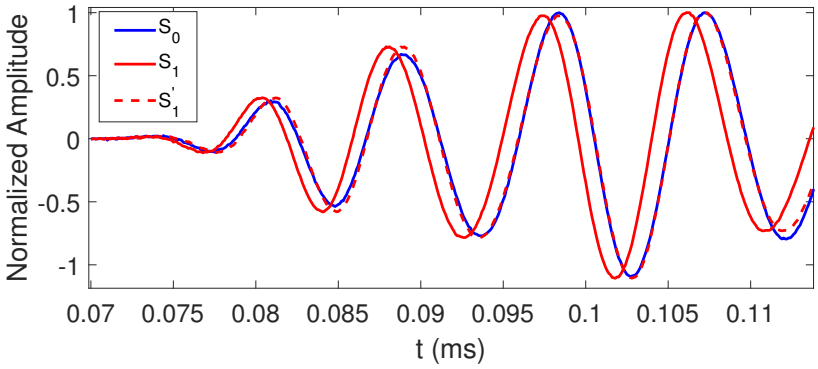

Figure 1. Stretching technique on two ultrasonic signals acquired from a stress-free state S_0, and a stressed state S_1. The red dash line is the stretched and interpolated signal S_1' with stretching parameter ε_{max}.

According to Snieder's research [6], for a Poisson medium, the CWI analysis result is primarily affected by the wave velocity variation of S waves. Therefore, in the case of homogeneous velocity changes, the CWI analysis result is close to the S wave-velocity change. On the other hand, if the velocity change is inhomogeneous, the CWI analysis result may depend on the selected time window positions of the signal. This difference has been explained theoretically by many researchers in their studies [7–10], and the time-dependency of sensitivity kernels may be used to image local changes in media.

The heterogeneous structure of concrete promotes rapid formation of a diffuse field. Therefore, CWI has been used to investigate small velocity changes induced by the acoustoelastic effect or nonlinear ultrasonic waves in concrete. Larose and Hall [11] reported the CWI technique could give a resolution of 2×10^{-5} relative wave-velocity change in concrete induced by uniaxial stress. Payan et al. [12] extracted the third-order elastic constants in concrete by measuring dV/V in different propagation and polarization directions under uniaxial stress. CWI also shows advantages in nondestructive evaluation (NDE) for very slow and weak changes in the material. For example, Liu et al. [13] used the CWI method to monitor the self-healing process of internal cracks in biomimetic mortar due to the biomineralization effect. Their experimental results clearly showed that the biomimetic samples cured with nutrition spray demonstrated a higher velocity increase than other test groups. Recently, Sun and Zhu [14] developed a nonlinear thermal modulation ultrasonic test for concrete damage evaluation by measuring the sensitivity of relative velocity changes to temperature variations. They also used this method to determine the absolute values of nonlinear acoustic parameters α, β, δ by using the temperature change as a driving force of nonlinear response of materials [15]. Zhong and Zhu [16] derived the theoretical formulas and validated this method on metals. In all the references reviewed above, the CWI method can measure very small wave-velocity changes, which would not be accurately measured using the conventional time of flight method.

Many studies used CWI for the measurement of velocity variation in the uniaxial loading test to investigate the acoustoelastic effect in concrete or rock [11,12,17–20]. Because the uniaxial loading test causes inhomogeneous stress field and velocity change in the concrete, CWI analysis results vary with the selected time windows in the signals.

Grêt et al. [17] found the relative wave-velocity changes at different time windows varied between 0.7% and 1.28 % in Berea sandstone due to a uniaxial stress increase of 2 MPa. Payan et al. [12] also reported varying values of dV/V when determining the third-order elastic constants in concrete using CWI analysis. In both studies, these authors calculated the mean values of velocity variations obtained in different time windows. Deraemaeker and Dumoulin [21] applied the stretching technique to the direct wave instead of the coda wave in a concrete beam loading test, where the end of the direct wave was based on the observation that signals did not show significant changes before cracking occurred. Zhan et al. [18] directly calculated the velocity changes using full coda waveforms instead of a specific part to remove the time dependence. It can be seen that researchers adopted different time windows in CWI analysis, while some results are significantly affected by the time window selection.

With an increasing research interest in coda wave analysis and wide applications of CWI for NDE of concrete, the authors believe there is a need to discuss time window effects on CWI analysis results, and extend CWI to direct wave analysis before diffuse wavefield forms in the medium. Direct wave velocities are often needed in nonlinear ultrasonic analysis and determination of elastic constants. This paper presents three applications of wave velocity monitoring in concrete: (1) early-age hydration, (2) temperature change, and (3) uniaxial loading. In all experiments, the stretching method is applied to the direct waves to extract the relative velocity changes of the direct P wave and S wave in concrete, which are compared with the CWI analysis results. It is found that the CWI cannot be used to determine the third-order elastic constants or acoustoelastic coefficients because coda wave does not maintain clear wave propagation and polarization directions.

2. Early-Age Concrete

Since the 1980s, ultrasonic wave velocity has been used to monitor early-age cement-based materials to predict the setting time and early-age strength development [22–25]. In most cases, the time of flight (TOF) of ultrasonic P or S waves was used to determine the wave velocity. Ultrasonic wave velocities in fresh concrete show a rapid increase during the first 24 h and gradually approach a constant value. The TOF method has sufficient resolution to monitor the concrete hydration process at a very early age (before 24 h), but it then becomes difficult to accurately track the velocity change after 24 h. In this section, the relative wave-velocity change was monitored in concrete after 24 h using the stretching technique.

Cement hydration leads to homogeneous changes of concrete properties, including strength, elastic modulus, and wave velocities, which all increase with concrete age. The P wave velocity V_p and S wave velocity V_s in elastic media can be expressed as:

$$V_p = \sqrt{\frac{E(1-\nu)}{\rho(1+\nu)(1-2\nu)}} \tag{2}$$

$$V_s = \sqrt{\frac{E}{2\rho(1+\nu)}} \tag{3}$$

where ρ is the mass density, ν is Poisson's ratio, and E is the modulus of elasticity. The ratio between V_p and V_s depends on Poisson's ratio.

A concrete cylinder with a diameter of 100 mm and a height of 200 mm was used for ultrasonic monitoring. The concrete cylinder was demolded after 24 h of mixing, and then two piezoelectric (PZT) discs (10 × 2 mm) were installed on the two opposite flat ends of the cylinder as the ultrasonic transmitter and receiver. An Olympus 5077PR ultrasonic square wave pulser/receiver was used to drive the PZT transmitter. The pulse duration was set for optimum driving at around 100 kHz. The received signals were acquired by a digital oscilloscope PicoScope® 4824 at the sampling rate of 40 MS/s, and the duration of each signal was 1 ms. Each signal was averaged ten times to increase the signal-to-noise

ratio. The ultrasonic signals were recorded every 20 min during 30–115 h of concrete age. Figure 2 illustrates the ultrasonic monitoring test setup.

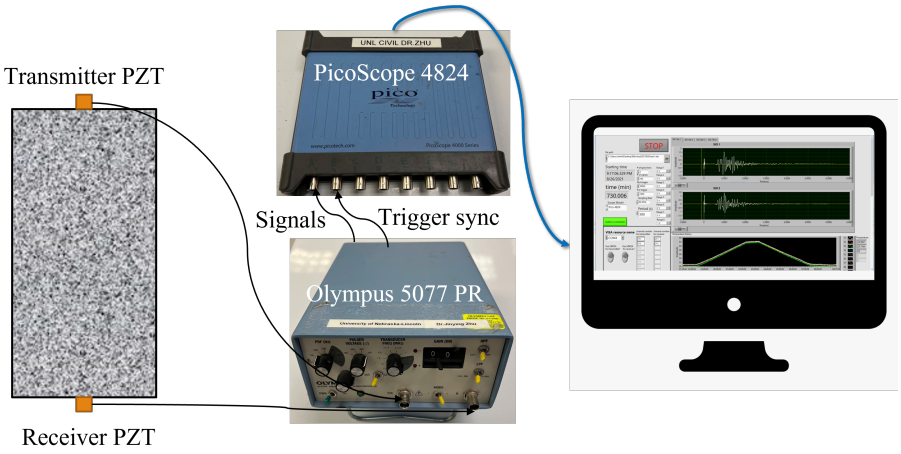

Figure 2. Schematic diagram illustrating the experimental setup for ultrasonic monitoring in all experiments. Additional sensors (thermocouple or load cell) were added in the temperature change and uni-axial loading test.

Figure 3 shows two ultrasonic signals recorded at the 75th hour and 80th hour of concrete age. The two insets of the figure show the details of the early part and the coda part of the signals. Since velocity change becomes very slow at this age, the two signals are almost identical in the early part, and it is challenging to accurately measure the change of TOF based on the first arrivals of a signal. The coda parts, instead, show a clear time shift. The red signal (80 h) is ahead of the blue signal, indicating an increase in velocity with concrete age. The P wave and S wave are dominant in the early time windows before 0.2 ms. The P wave part signal is within the time range of $t_p \sim 1.5t_p$ before the direct S wave arrival. Because the PZT discs vibrate in the radial mode, a strong S wave is generated and it can be clearly distinguished from the P wave signal. Although the P wave part may contain a small amount of mode-converted S wave energy, and the S wave part contains some P wave energy, each window is dominated by P and S wave energy, respectively. In these short time windows, The relative velocity change dV/V calculated through cross-correlation analysis is determined by the dominating wave component. Therefore, dV/V calculated in the P and S wave windows can be regarded as the relative velocity change of P and S waves.

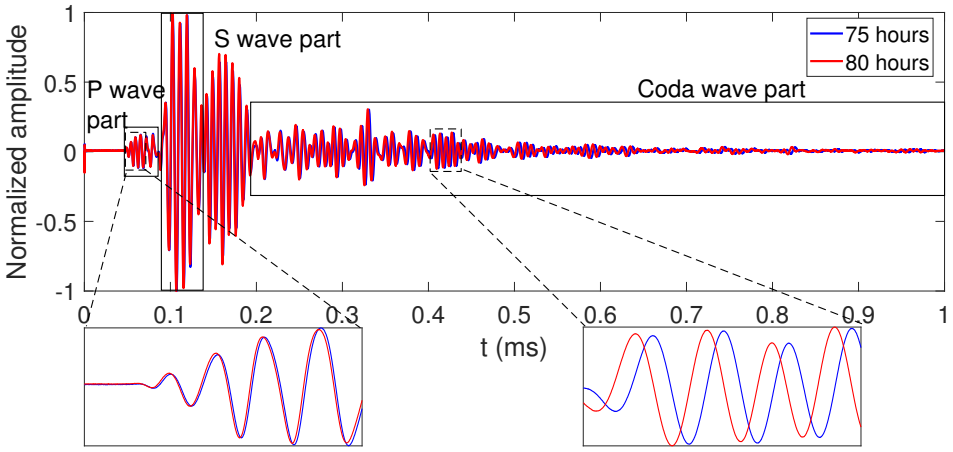

Figure 3. Two ultrasonic signals recorded at ages of 75 and 80 h. The insets show large time shift in the coda wave.

To show the overall trend of velocity change with age, all signals are stacked together to form an image with axes of signal time (horizontal) and concrete age (vertical), as shown in Figure 4. This method has been used by Zhu et al. [26,27] to manually trace the P or S wave arrivals based on the trend of waveforms. It can be seen that the P wave arrival times (very early part before 0.09 ms) show very little change during the entire monitoring period, while the coda waves show a clear and measurable time shift with aging. The coda wave has a similar changing trend to the S wave but becomes more pronounced at a later time, and the coda wave signals still maintain a good correlation (clear trend) during the entire monitoring period.

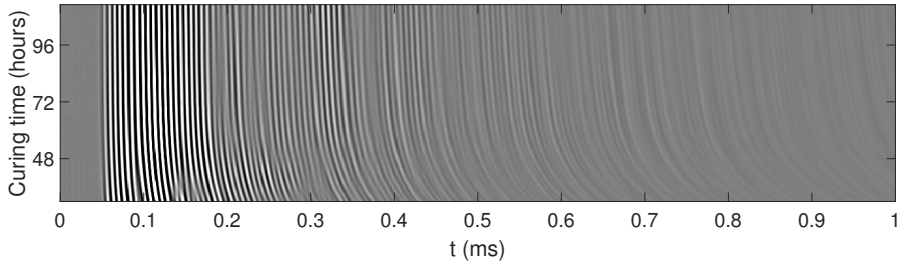

Figure 4. Stacked ultrasonic signal image shows the trend of time shifts in early-age concrete.

Figure 5 gives the calculated relative wave-velocity change between signals recorded at ages of 75th hour and 80th hour. A moving time window with a width of 0.1 ms and a step of 0.05 ms is used for stretching analysis. It can be seen that different time windows give the same dV/V results. The cross-correlation coefficient $CC(\varepsilon_{max})$ calculated at each moving time window is above 0.99, which indicates a very weak distortion between these two signals.

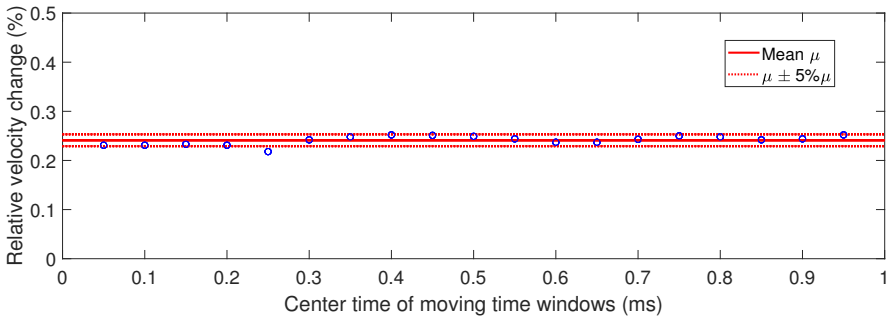

Figure 5. Relative velocity change calculated at different time window locations, between two signals collected at the 75th and 80th hours.

To study the window effect, the stretching method was applied to four time windows for all signals: P wave part, S wave part, coda wave part, and the full-length signal to measure the velocity change during concrete hydration. Figure 6 shows the relative velocity change calculated from the four time windows. All curves indicate that the wave velocities increase with the age of concrete. Similar results were obtained on the coda wave, full-length signals, and the S wave windowed signals. This result is consistent with the conclusions given by Weaver [28], and Snieder [6] that the S wave energy dominates the diffuse wave. P wave has a smaller dV/V than S wave, which supports conclusions from previous studies [29–31]: the relative S wave velocity increases faster than the P wave velocity during the early-age-cement-hydration stages. This phenomenon is related to the microstructure development in early concrete. Continued cement hydration contributes to the formation of the solid phase which increases the shear modulus and shear wave velocity, while the P wave velocity is affected to a lesser degree because the P wave can propagate in both the fluid and solid phases.

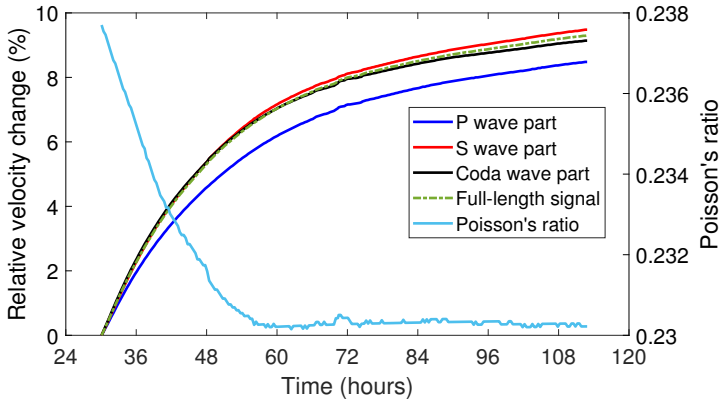

Figure 6. Relative wave velocity changes and Poisson's ratio development calculated from different time windows. The reference signal was obtained at 30 h.

It is well known that Poisson's ratio decreases when fresh concrete changes from a fluid-like state to a solid state. Although Poisson's ratio can be calculated from the ratio of V_p to V_s, the very slow change of velocities after 24 h of concrete age will induce large errors in wave velocity measurements and Poisson's ratio calculation. At a very early age t_0, the wave velocities (V_{p0}, V_{s0}) can be measured with relatively small errors due to large travel times, and a reference Poisson's ratio ν_0 could be reliably determined. Then ν_1 at a later age can be calculated based on the relative velocity change in P wave and S wave using the following relationship (Equation (4)):

$$\frac{1-\nu_1}{1-2\nu_1} = \frac{V_p^2}{2V_s^2} = \frac{(1+\Delta V_p/V_{p0})^2}{(1+\Delta V_s/V_{s0})^2}\frac{1-\nu_0}{1-2\nu_0} \tag{4}$$

In this study, we used the P wave and S wave velocities at 30 h in the concrete cylinder as a reference, which were 4211 m/s and 2470 m/s. The Poisson's ratio is calculated as 0.238 using Equation (5)

$$\nu = \frac{V_p^2 - 2V_s^2}{2\left(V_p^2 - V_s^2\right)} \tag{5}$$

Figure 6 also shows the development of Poisson's ratio with concrete age up to 5 days. The Poisson's ratio decreases from 0.238 at 30 h to 0.23 at 58 h and then stays constant. The change of Poisson's ratio in concrete is very small (less than 5%) after 30 h, which agrees with the result in reference [30]. By applying the stretching technique analysis to signal windows dominated by P and S waves, the changes of wave velocities and Poisson's ratio can be calculated with an improved accuracy compared to the TOF method.

Because hydration-induced property change is homogeneous in concrete, the stretching technique method can be applied successfully to the coda wave part (CWI) to estimate shear wave-velocity change, and window positions have very little effect on the result. In the study of Liu et al. [32], the S wave velocity proved to be a more reliable indicator than the P wave velocity for the monitoring of the setting and hardening process of cementitious materials. Unlike the P wave, the exact arrival time of the S wave is difficult to determine. From our experimental results, the wave-velocity change of the coda wave can be used to represent S wave-velocity change with high resolution.

3. Temperature Effect

Temperature change has significant effects on ultrasonic wave velocities in metals, rock, and concrete [14,17,33,34]. Temperature effects are commonly considered as an undesired noise in ultrasonic measurements. Zhang et al. [19] proposed using a reference sample identical to the test sample to compensate for the temperature change effect. However, a reference sample is not always available in engineering practice, and the temperature

effects on the reference are not always the same as in the test structure. Recently, Sun and Zhu [15] used the relationship between wave velocity and temperature to determine the acoustic nonlinearity parameters, and evaluate concrete samples with alkali-silica reaction (ASR) damage. They found that the damaged concrete samples showed higher sensitivity to temperature than the control samples. In their study, CWI was used to determine the relative wave-velocity change with temperature.

Weaver [33] reported that the temperature dependence of wave velocity is different for P wave and S wave. Because the relative contributions of P and S waves vary with time window positions in a signal, the CWI analysis results also vary with window positions. This section presents the application of the stretching technique to different parts of signals and the results are compared.

Similar to the test setup in Section 2, two PZT discs (10 × 2 mm) were attached to the opposite flat ends of a concrete cylinder at a distance of 200 mm. The P wave velocity of the concrete cylinder was measured at 4600 m/s, and the compressive strength was 48 MPa. Ultrasonic signals of 1.8 ms duration were acquired every 2 min. Another concrete cylinder containing a surface and an internal thermocouple was used to monitor the temperature changes during the measurement. These two concrete cylinders were placed in an environmental chamber for heating at a temperature-change rate of 1 °C/h to avoid a large thermal gradient. Figure 7 shows two ultrasonic signals acquired at 27 °C and 29 °C. It can be seen that the latter part shows larger time shifts than the early part of the signal. The stretching technique was applied to the following signal window positions: P wave part, S wave part, full-length signal, and moving time windows. Determination of P and S wave parts still follows the same procedure as in the early-age concrete test.

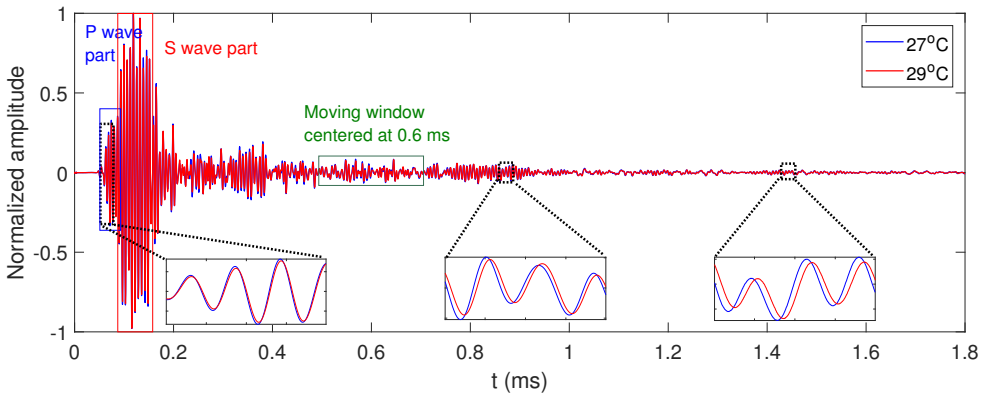

Figure 7. Two ultrasonic signals collected at 27 °C and 29 °C. Three zoomed insets show the time shifts at different window locations.

Figure 8 presents the relative velocity change vs. temperature variation using different time windows. It should be noted that the calculated slope values α in Figure 8 include the thermal expansion effect. The relative time shift dt/t or velocity change dV/V calculated using the stretching technique method includes two components: temperature-induced velocity change and length change caused by thermal expansion. The actual temperature-induced relative velocity change is $dV/V - \alpha_T \Delta T$, after correction of thermal expansion induced length change (thermal strain), where α_T is the coefficient of thermal expansion. The stretching analyses on the full-length signal and the S wave part give very close results, which is consistent with the theory that CWI is more sensitive to perturbations on the S wave velocity than on the P wave velocity [6]. Snieder also showed that the relative velocity change of the coda wave is the weighted average of the P and S velocity perturbation given by

$$\frac{dV}{V} = 0.09\frac{dV_p}{V_p} + 0.91\frac{dV_s}{V_s} \quad (6)$$

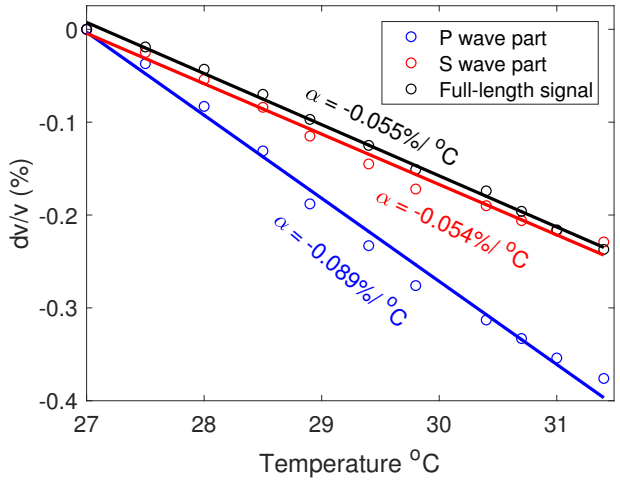

Figure 8. Relative velocity changes of P and S waves with temperature.

Figure 9 shows the calculated $\alpha = dV/V/\Delta T$ for different time window positions. A time window of 0.2 ms wide moved from 0.2 ms to 1.6 ms (center) with a step of 0.1 ms. The first three data points represent results from the windowed P and S waves, and the full-length signals. The P wave velocity has a larger change (-0.089%) than the S wave velocity (-0.054%), while the S wave, the coda, and the full-length signal give similar results. This result is not surprising because the full-length signal is dominated by the high amplitude of the S wave. The coda wave-velocity change is slightly larger than the S wave change and agrees with the weighted average of 0.058% calculated from Equation (6).

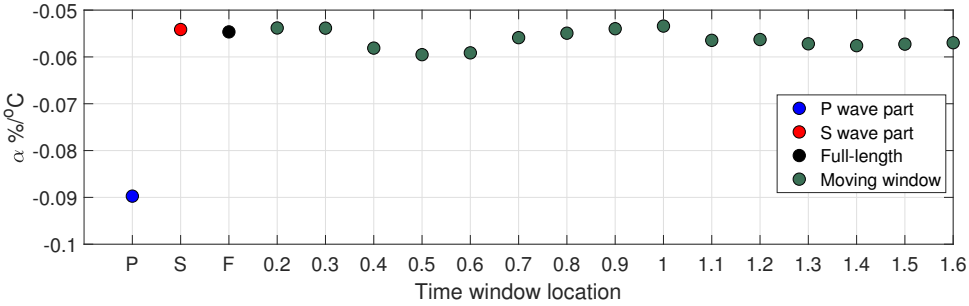

Figure 9. Calculated $\alpha = dV/V/\Delta T$ using different time windows. Time window locations P, S, and F represent the direct P wave, S wave, and full-length signal. Other time window locations represent a 0.2 ms wide moving window centered from 0.2 ms to 1.6 ms with a step of 0.1 ms.

4. Concrete Subject to Uniaxial Stress

Acoustoelastic effect [35,36] refers to the linear relation between wave velocities and stress in elastic materials. Under the uniaxial stress σ_{11}, the wave velocities can be expressed as (to the first order) [37]:

$$V_{ij}^{\sigma} = V_{ij}^{0}(1 + \alpha_{ij}\sigma_{11}) \tag{7}$$

where V_{ij}^{σ} is the wave velocity under the uniaxial stress σ_{11}, and V_{ij}^{0} is the wave velocity under a stress-free state. The subscript ij stands for the wave propagation direction and polarization direction. α_{ij} is defined as the acoustoelastic coefficient, which depends on the second- and third-order elastic constants (Lamé and Murnaghan constants), wave propagation, and polarization directions.

In this study, we measured acoustoelastic coefficients on a 100 mm $\times$ 200 mm concrete cylinder. The concrete cylinder has a compressive strength of 55 MPa, and a P wave velocity

of 4650 m/s. The experimental setup is shown in Figure 10. Three PZT discs (10 × 2 mm) were installed on the surface of the cylinder using epoxy. One PZT disc was used as an ultrasonic transmitter, and two other PZT discs were receivers, as shown in the figure. The receivers are named the transverse receiver (⊥ receiver) and the parallel receiver (// receiver) based on the wave propagation directions relative to the loading direction. The source-receive spacing was 100 mm in the transverse direction and 60 mm in the parallel direction. The concrete cylinder was preloaded to 8 MPa for one cycle to make it stable for the following loading and ultrasonic measurement. After preloading, the concrete cylinder was loaded at a rate of 20 kPa/second to 8 MPa and then unloaded, for three cycles. A load cell was placed under the concrete cylinder to record the loading process.

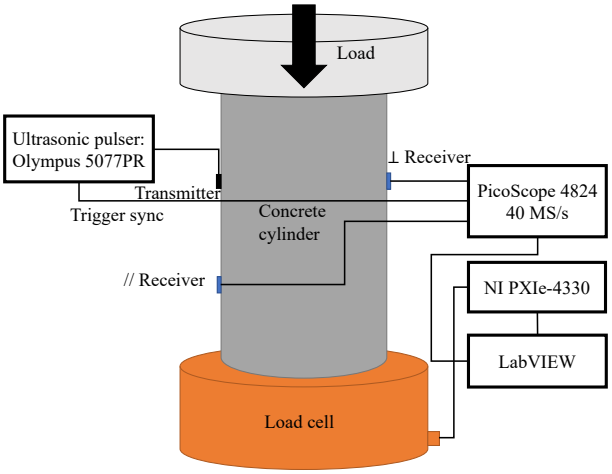

Figure 10. Experimental setup of uniaxial loading test on a 100 mm × 200 mm concrete cylinder.

The ultrasonic measurement setup was similar to that used in the previous early-age concrete and temperature effect tests, with some modifications to sampling parameters. Signals were sampled at 40 MS/s with a duration of 1.6 ms and recorded at an interval of 2 s during the loading process. Each signal was averaged ten times to increase the signal-to-noise ratio. A LabVIEW program was developed to control the data acquisition system and synchronize ultrasonic data and loading data. An example signal received by the parallel receiver is shown in Figure 11.

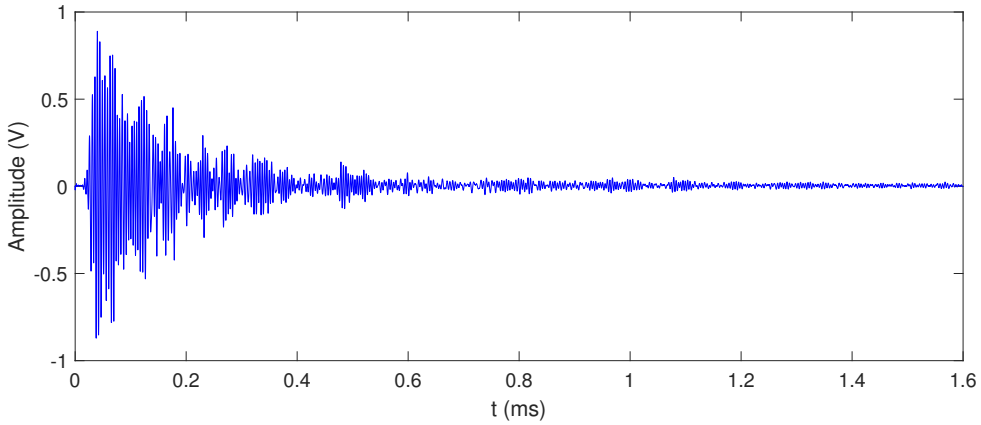

Figure 11. A typical ultrasonic signal received by the parallel receiver.

To clearly show the time shift trend with stress, we first extract all zero-crossing points from the signals, and then connect the zero-crossing points to form an image, as shown in Figure 12. The horizontal axis represents signal time, and the vertical axis represents loading steps, with corresponding stress shown to the left. Figure 12a,b present the signal images, which give the first arrival times of 0.013 ms and 0.02 ms for the parallel and

transverse receivers, respectively. The time shifts in both directions follow the trend of stress variation, but their sensitivities and coherence vary with the time window. Overall, the time shift becomes more pronounced with increasing signal time. When the time shifts become too large or signals show large distortions, the images do not show good correlations with the stress pattern, such as in the window [0.14, 0.175] ms in Figure 12a, and [0.145, 0.185] ms in Figure 12b.

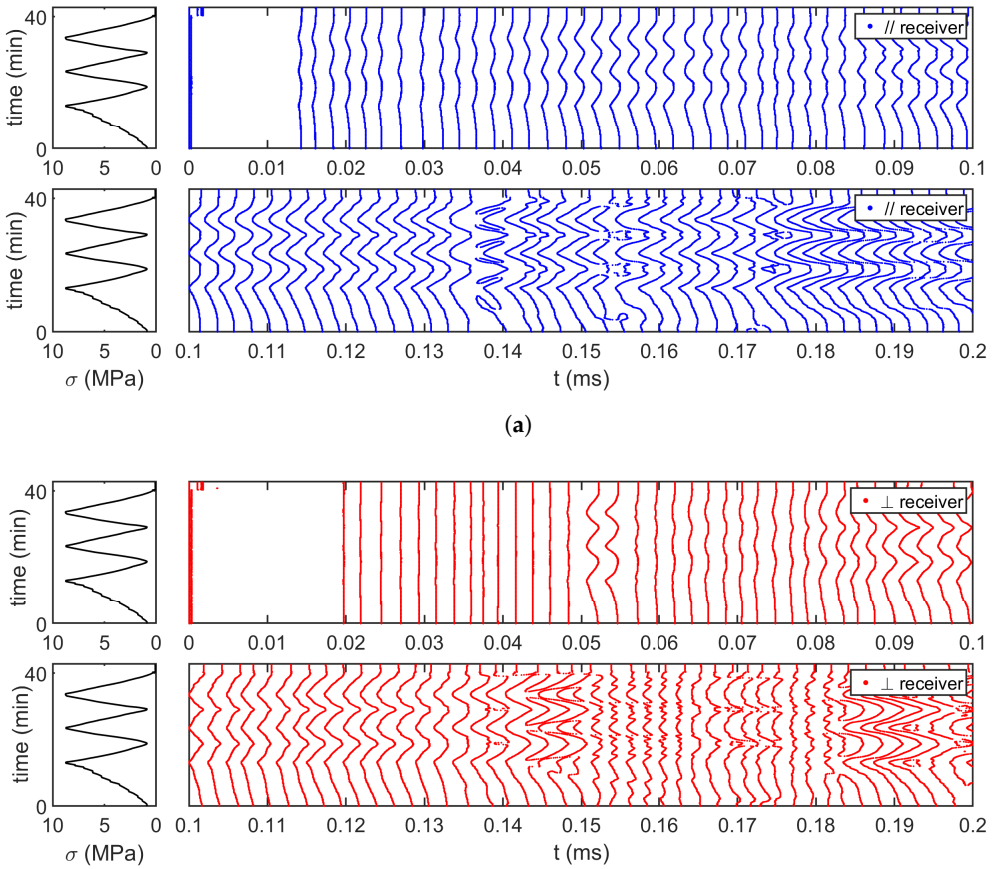

Figure 12. Zero-cross images of ultrasonic signals show time shifts in the parallel direction and transverse direction with uniaxial stress change. The horizontal axis represents signal time, and the vertical axis represents load steps for a duration of 40 min, with corresponding stress on the left. (**a**) Parallel direction; (**b**) Transverse direction.

Figure 13 shows the relative velocity change vs. stress by analyzing the direct P wave and full-length signals in the parallel and transverse directions. Only the results from the first loading cycle are presented because the three loading cycles give similar results. The relative velocity change dV_{11}/V_{11} of the P wave in the parallel direction shows the highest sensitivity (0.268%/MPa) to stress change when the wave propagation and polarization directions align with the stress direction. P wave velocity has the least sensitivity in the transverse direction (dV_{22}/V_{22} = 0.023%/MPa). These results agree with previous findings by other researchers [37,38]. However, if the full-length signals were analyzed, the acoustoelastic coefficients calculated from both directions would become very close (0.121%/MPa and 0.105%/MPa). The P wave velocity in the transverse direction was expected to decrease with stress owing to Poisson's effect, but it increased in the uniaxial loading experiment. This behavior was also observed in other studies [37]. The authors believe this phenomenon was caused by the circumferential restraint due to end zone friction when the concrete cylinder is under compression [39,40].

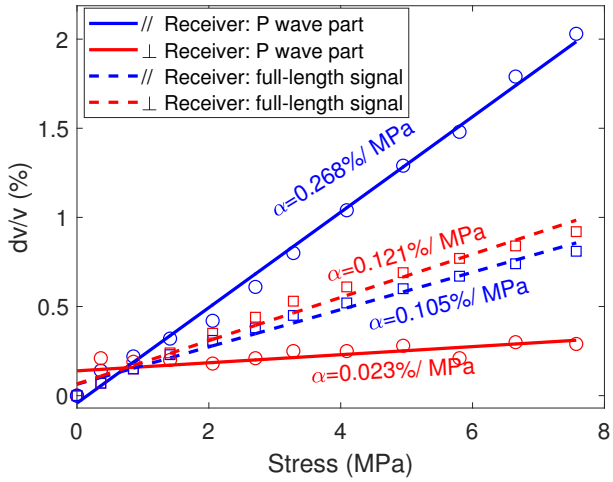

Figure 13. Relative velocity change vs. stress by applying stretching technique to the P wave part and full-length signals in parallel and transverse directions.

To investigate the time window effects on measurements of acoustoelastic coefficients, a moving time window with a width of 0.2 ms was used for stretching technique analysis. The center time of the window moved from 0.1 ms to 1.5 ms. Figure 14 summarizes the calculated acoustoelastic coefficients in both directions using different time windows. For a time window before 0.25 ms, the acoustoelastic coefficients measured in two directions have a clear difference, and α_{11} in the parallel direction is larger than α_{22} in the transverse direction. After 0.25 ms, which is more than ten times the first arrival time (0.015 to 0.02 ms), the calculated acoustoelastic coefficients in both directions become very close. This indicates that the coda wave does not show directivity toward the stress direction. Although the coda wave velocity still increases with stress level (positive α), which is similar to the full-length signal result in Figure 13, the α value measured from the coda wave or full-length signal is different from α_{11} and any acoustoelastic coefficient α_{ij} in Equation (7).

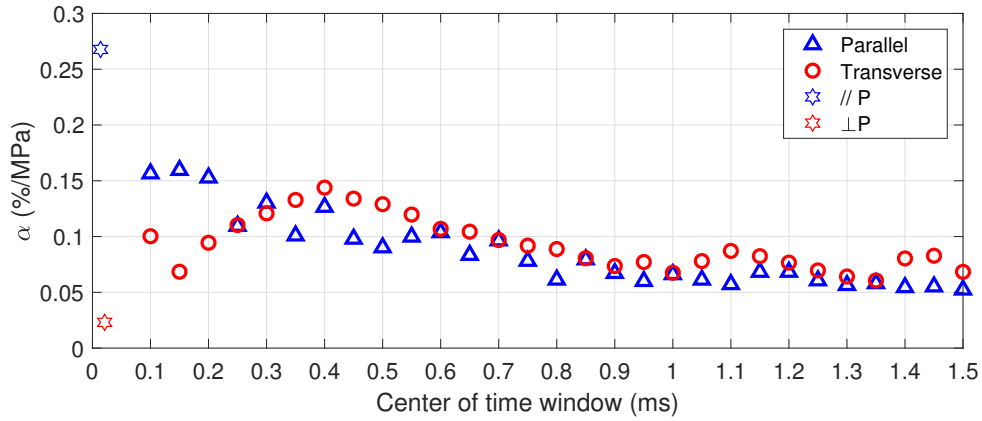

Figure 14. Calculated acoustoelastic coefficients in two directions at different time windows. The window center moves from 0.1 ms to 1.5 ms with a window width of 0.2 ms. The first data point represents the stretching technique analysis on the P wave signals.

Compared to the concrete hydration and temperature change experiments, the relative velocity change due to uniaxial loading shows more variation. Weak anisotropy caused by the uniaxial stress results in non-uniform strain and wave-velocity changes in different time windows. In a uniaxial experiment on a concrete cylinder, Payan et al. [12] also noticed large fluctuations of CWI calculated dV/V with window positions.

Lillamand et al. [37], Bompan and Haach [38] reported that the acoustoelastic effect was the most significant when the wave propagated and polarized in the stress direction.

Therefore, the P wave propagating in the stress direction shows the largest velocity change. However, if the full-length signals are analyzed, the relative velocity changes do not show much difference between two directions. In the cylinder test, the acoustoelastic coefficients were $\alpha_{11} = 0.105$ %/MPa in the stress direction, and $\alpha_{22} = 0.121$ %/MPa in the non-stress direction, respectively. After multiple scatterings, the fully diffused wave has random propagation and polarization directions, and they no longer follow the direct wave path. Signals at different windows contain different wave types, polarization, and propagation directions, which causes variations in the relative velocity change calculation. Therefore, the relative velocity changes dV/V calculated from the coda wave or the full-length signal cannot be used to calculate the corresponding acoustoelastic coefficients.

In theory, the acoustoelastic effect may be used for stress evaluation in concrete by comparing the velocity difference between the stressed and non-stressed conditions. However, it is very difficult to accurately measure the very small velocity difference between different concrete samples due to the heterogeneity and large variation of concrete properties. Results presented in this study provide a potential solution by measuring the in situ velocity difference between two directions (α_{11} and α_{22}) on the same concrete structure member, which reduces the material variations and temperature effect. For this purpose, the stretching technique should be applied to the direct P wave part signals in the stressed and the non-stressed directions. This approach has been applied to a full-scale concrete bridge girder to monitor the prestress release process by the authors [20].

5. Conclusions

The stretching technique and CWI have been used to measure minor wave-velocity changes in concrete. Their high sensitivity has attracted much research interest in different NDE applications, including evaluation of microcracking damage, healing, stress estimation, temperature effects, etc. However, many researchers starting in this field are often confused about the interpretation of the CWI results. In this study, we present three experimental cases for application of the stretching technique: early-age hydration, temperature change, and uniaxial compressive loading. The first two cases cause homogeneous velocity change. Based on the experimental results, the following conclusions can be drawn:

1. In very early-age concrete, the P and S wave arrivals can be easily determined using the first arrivals with little error; but after 24 h, the measurement error will increase when the wave arrivals become short and their changes become very slow. Using the P and S wave arrivals at a very early age as the reference values, the stretching technique can then be used to track the changes of wave velocities and Poisson's ratio with high accuracy after 24 h. Because the material property change is homogeneous, stretching analyses concerning the coda wave, the S wave, and the full-length signal give similar results. The stretching technique provides an easy solution to accurately monitor the S wave-velocity change in early-age concrete.
2. Uniform temperature change causes homogeneous velocity change in the concrete, so stretching analysis on the coda wave gives consistent results for different time windows. The P and S wave-velocity change can be calculated by applying the stretching procedure to P and S wave part signals only. If the signal does not show a clear S wave pulse, the S wave-velocity change may be derived from Equation (6). The relative velocity changes dV_p/V_p and dV_s/V_s due to temperature change can be used to calculate the third-order elastic constants in concrete [16].
3. Uniaxial compressive loading generates non-uniform strain field and velocity changes in concrete. Therefore, the stretching result of the coda wave varies with the window time and does not show directivity to the stress direction. This is because the diffuse wave has random propagation and polarity directions due to multiple scattering in the medium.
4. In order to measure acoustoelastic coefficients or third-order elastic constant using the uniaxial loading test, we must use direct P or S waves which maintain clear propagation and polarity direction. The direct waves give different dV/V along

with the stressed (11) and non-stressed (22) directions. This property may be used to evaluate the stress level in large prestressed concrete structural members [20].

Author Contributions: Conceptualization, methodology B.Z. and J.Z.; software, formal analysis, resources, data curation, investigation, writing—original draft preparation B.Z.; writing—review and editing, supervision, funding acquisition, J.Z. All authors have read and agreed to the published version of the manuscript.

Funding: This research was funded by the Nebraska Department of Transportation (NDOT), United States.

Institutional Review Board Statement: Not applicable.

Informed Consent Statement: Not applicable.

Data Availability Statement: The data that support the findings of this study are available from the corresponding author upon reasonable request.

Acknowledgments: The authors would like to acknowledge the NDT-CE team members at the University of Nebraska-Lincoln for their help in preparing concrete specimens.

Conflicts of Interest: The authors declare no conflict of interest.

References

1. Snieder, R.; Grêt, A.; Douma, H.; Scales, J. Coda Wave Interferometry for Estimating Nonlinear Behavior in Seismic Velocity. *Science* **2002**, *295*, 2253–2255. [CrossRef] [PubMed]
2. Snieder, R. The theory of coda wave interferometry. *Pure Appl. Geophys.* **2006**, *163*, 455–473. [CrossRef]
3. Planès, T.; Larose, E. A review of ultrasonic Coda Wave Interferometry in concrete. *Cem. Concr. Res.* **2013**, *53*, 248–255. [CrossRef]
4. Lobkis, O.I.; Weaver, R.L. Coda-Wave Interferometry in Finite Solids: Recovery of P-to-S Conversion Rates in an Elastodynamic Billiard. *Phys. Rev. Lett.* **2003**, *90*, 254302. [CrossRef]
5. Hadziioannou, C.; Larose, E.; Coutant, O.; Roux, P.; Campillo, M. Stability of monitoring weak changes in multiply scattering media with ambient noise correlation: Laboratory experiments. *J. Acoust. Soc. Am.* **2009**, *125*, 3688–3695. [CrossRef]
6. Snieder, R. Coda wave interferometry and the equilibration of energy in elastic media. *Phys. Rev. E* **2002**, *66*, 046615. [CrossRef]
7. Obermann, A.; Planes, T.; Larose, E.; Sens-Schönfelder, C.; Campillo, M. Depth sensitivity of seismic coda waves to velocity perturbations in an elastic heterogeneous medium. *Geophys. J. Int.* **2013**, *194*, 372–382. [CrossRef]
8. Planès, T.; Larose, E.; Margerin, L.; Rossetto, V.; Sens-Schoenfelder, C. Decorrelation and phase-shift of coda waves induced by local changes: Multiple scattering approach and numerical validation. *Waves Random Complex Media* **2014**, *24*, 99–125. [CrossRef]
9. Planès, T.; Larose, E.; Rossetto, V.; Margerin, L. Imaging multiple local changes in heterogeneous media with diffuse waves. *J. Acoust. Soc. Am.* **2015**, *137*, 660–667. [CrossRef]
10. Margerin, L.; Planès, T.; Mayor, J.; Calvet, M. Sensitivity kernels for coda-wave interferometry and scattering tomography: Theory and numerical evaluation in two-dimensional anisotropically scattering media. *Geophys. J. Int.* **2016**, *204*, 650–666. [CrossRef]
11. Larose, E.; Hall, S. Monitoring stress related velocity variation in concrete with a 2×10^{-5} relative resolution using diffuse ultrasound. *J. Acoust. Soc. Am.* **2009**, *125*, 1853–1856. [CrossRef] [PubMed]
12. Payan, C.; Garnier, V.; Moysan, J.; Johnson, P. Determination of third order elastic constants in a complex solid applying coda wave interferometry. *Appl. Phys. Lett.* **2009**, *94*, 011904. [CrossRef]
13. Liu, S.; Bundur, Z.B.; Zhu, J.; Ferron, R.D. Evaluation of self-healing of internal cracks in biomimetic mortar using coda wave interferometry. *Cem. Concr. Res.* **2016**, *83*, 70–78. [CrossRef]
14. Sun, H.; Zhu, J. Thermal modulation of nonlinear ultrasonic wave for concrete damage evaluation. *J. Acoust. Soc. Am.* **2019**, *145*, EL405–EL409. [CrossRef] [PubMed]
15. Sun, H.; Zhu, J. Determination of acoustic nonlinearity parameters using thermal modulation of ultrasonic waves. *Appl. Phys. Lett.* **2020**, *116*, 241901. [CrossRef]
16. Zhong, B.; Zhu, J. Measurement of third-order elastic constants using thermal modulation of ultrasonic waves. *Appl. Phys. Lett.* **2021**, *118*, 261903. [CrossRef]
17. Grêt, A.; Snieder, R.; Scales, J. Time-lapse monitoring of rock properties with coda wave interferometry. *J. Geophys. Res. Solid Earth* **2006**, *111*. [CrossRef]
18. Zhan, H.; Jiang, H.; Zhuang, C.; Zhang, J.; Jiang, R. Estimation of Stresses in Concrete by Using Coda Wave Interferometry to Establish an Acoustoelastic Modulus Database. *Sensors* **2020**, *20*, 4031. [CrossRef]
19. Zhang, Y.; Abraham, O.; Tournat, V.; Le Duff, A.; Lascoup, B.; Loukili, A.; Grondin, F.; Durand, O. Validation of a thermal bias control technique for Coda Wave Interferometry (CWI). *Ultrasonics* **2013**, *53*, 658–664. [CrossRef]
20. Zhong, B.; Zhu, J.; Morcous, G. Measuring acoustoelastic coefficients for stress evaluation in concrete. *Constr. Build. Mater.* **2021**, *309*, 125127. [CrossRef]

21. Deraemaeker, A.; Dumoulin, C. Embedding ultrasonic transducers in concrete: A lifelong monitoring technology. *Constr. Build. Mater.* **2019**, *194*, 42–50. [CrossRef]
22. Krauß, M.; Hariri, K. Determination of initial degree of hydration for improvement of early-age properties of concrete using ultrasonic wave propagation. *Cem. Concr. Compos.* **2006**, *28*, 299–306. [CrossRef]
23. Robeyst, N.; Gruyaert, E.; Grosse, C.U.; De Belie, N. Monitoring the setting of concrete containing blast-furnace slag by measuring the ultrasonic p-wave velocity. *Cem. Concr. Res.* **2008**, *38*, 1169–1176. [CrossRef]
24. Desmet, B.; Atitung, K.C.; Abril Sanchez, M.A.; Vantomme, J.; Feys, D.; Robeyst, N.; Audenaert, K.; De Schutter, G.; Boel, V.; Heirman, G.; et al. Monitoring the early-age hydration of self-compacting concrete using ultrasonic p-wave transmission and isothermal calorimetry. *Mater. Struct.* **2011**, *44*, 1537–1558. [CrossRef]
25. Rybak, J. Non-destructive determining of foundation pile length variability for reliability analysis. *J. Phys. Conf. Ser.* **2019**, *1425*, 012205. [CrossRef]
26. Zhu, J.; Kee, S.H.; Han, D.; Tsai, Y.T. Effects of air voids on ultrasonic wave propagation in early age cement pastes. *Cem. Concr. Res.* **2011**, *41*, 872–881. [CrossRef]
27. Zhu, J.; Tsai, Y.T.; Kee, S.H. Monitoring early age property of cement and concrete using piezoceramic bender elements. *Smart Mater. Struct.* **2011**, *20*, 115014. [CrossRef]
28. Weaver, R.L. On diffuse waves in solid media. *J. Acoust. Soc. Am.* **1982**, *71*, 1608–1609. [CrossRef]
29. Carette, J.; Staquet, S. Monitoring the setting process of eco-binders by ultrasonic P-wave and S-wave transmission velocity measurement: Mortar vs concrete. *Constr. Build. Mater.* **2016**, *110*, 32–41. [CrossRef]
30. Boumiz, A.; Vernet, C.; Tenoudji, F.C. Mechanical properties of cement pastes and mortars at early ages: Evolution with time and degree of hydration. *Adv. Cem. Based Mater.* **1996**, *3*, 94–106. [CrossRef]
31. Zhu, J.; Kee, S.H. Monitoring early age microstructure development of cement paste using bender elements. In Proceedings of the Nondestructive Characterization for Composite Materials, Aerospace Engineering, Civil Infrastructure, and Homeland Security 2010. International Society for Optics and Photonics, San Diego, CA, USA, 7–11 March 2010; Volume 7649, p. 76491R.
32. Liu, S.; Zhu, J.; Seraj, S.; Cano, R.; Juenger, M. Monitoring setting and hardening process of mortar and concrete using ultrasonic shear waves. *Constr. Build. Mater.* **2014**, *72*, 248–255. [CrossRef]
33. Weaver, R.L.; Lobkis, O.I. Temperature dependence of diffuse field phase. *Ultrasonics* **2000**, *38*, 491–494. [CrossRef]
34. Niederleithinger, E.; Wunderlich, C. Influence of small temperature variations on the ultrasonic velocity in concrete. In Proceedings of the AIP Conference Proceedings, Denver, CO, USA, 15–20 July 2012; American Institute of Physics: College Park, MD, USA, 2013; Volume 1511, pp. 390–397.
35. Murnaghan, F.D. *Finite Deformation of an Elastic Solid*; Wiley: Hoboken, NJ, USA, 1951.
36. Egle, D.; Bray, D. Measurement of acoustoelastic and third-order elastic constants for rail steel. *J. Acoust. Soc. Am.* **1976**, *60*, 741–744. [CrossRef]
37. Lillamand, I.; Chaix, J.F.; Ploix, M.A.; Garnier, V. Acoustoelastic effect in concrete material under uni-axial compressive loading. *NDT E Int.* **2010**, *43*, 655–660. [CrossRef]
38. Bompan, K.F.; Haach, V.G. Ultrasonic tests in the evaluation of the stress level in concrete prisms based on the acoustoelasticity. *Constr. Build. Mater.* **2018**, *162*, 740–750. [CrossRef]
39. Kotsovos, M. Effect of testing techniques on the post-ultimate behaviour of concrete in compression. *Matériaux Constr.* **1983**, *16*, 3–12. [CrossRef]
40. Kumar, S.; Mukhopadhyay, T.; Waseem, S.; Singh, B.; Iqbal, M. Effect of Platen Restraint on Stress–Strain Behavior of Concrete Under Uniaxial Compression: A Comparative Study. *Strength Mater.* **2016**, *48*, 592–602. [CrossRef]